

# Formation time of hadrons in photon induced reactions on nuclei\*

T. Falter and U. Mosel  
*Institut fuer Theoretische Physik*  
*Universitaet Giessen*  
*D-35392 Giessen, Germany*

February 11, 2002

## Abstract

We present a way to account for coherence length effects in a semi-classical transport model. This allows us to describe photo- and electroproduction at large nuclei ( $A > 12$ ) and high energies using a realistic coupled channel description of the final state interactions that goes far beyond simple Glauber theory. We show that the purely absorptive treatment of the final state interactions as usually done in simple Glauber theory might lead to wrong estimates of color transparency and formation time effects in particle production. As an example we discuss exclusive  $\rho^0$  photoproduction on Pb at a photon energy of 7 GeV as well as  $K^+$  and  $K^-$  production on C and Pb in the photon energy range 1-7 GeV.

## 1 Introduction

In a high energy collision between two hadrons or a photon and a hadron it takes a finite amount of time for the reaction products to evolve to physical particles. During the collision process some momentum transfer between the hadrons or some hard scattering between two of the hadrons' constituents leads to the excitation of hadronic strings. The time that is needed for the creation and fission of these strings as well as for the hadronization of the string fragments cannot be calculated within perturbative QCD because the hadronization process involves small momentum transfers of typically only a few hundred MeV. One can perform an estimate of the formation time  $\tau_f$  in the rest frame of the hadron. It should be of the order of the time that the quark-antiquark (quark-diquark) pair needs to reach a separation that is of the size of the produced hadron ( $r_h \approx 0.6 - 0.8$  fm):

$$\tau_f \gtrsim \frac{r_h}{c}. \quad (1)$$

During their evolution to physical hadrons the reaction products will react with reduced cross sections. This is motivated by means of color transparency: the strings and the substrings created during the

---

\*Work supported by DFG.

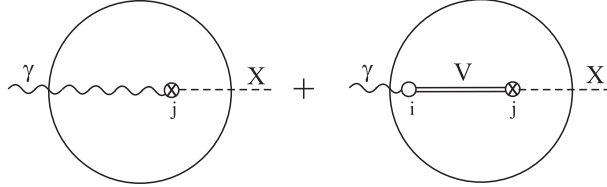


Figure 1: The two amplitudes of order  $\alpha_{em}$  that contribute to incoherent meson photoproduction in simple Glauber theory. The left amplitude alone would lead to an unshadowed cross section. Its interference with the right amplitude gives rise to shadowing.

fragmentation are in a color singlet state and therefore mainly react via their color dipole moment which is proportional to their transverse size. For a collision inside nuclear medium this means that during their formation time the produced hadrons travel with a reduced scattering probability. Hence the formation time plays an important role in the dynamics of nuclear reactions, e.g. heavy ion collisions, proton and pion induced reactions as well as photon and electron induced reactions on nuclei. The latter two are of special interest because they are less complex than heavy ion collisions and instead of hadron induced reactions the primary reaction does in general not only take place at the surface of the nucleus but also at larger densities. Experiments at TJNAF and DESY, for example, deal with exclusive and inclusive meson photo- and electroproduction at high energies. Large photon energies  $E_\gamma$  are of special interest because the formation length  $l_f$  in the rest frame of the nucleus can exceed nuclear dimensions:

$$l_f = v_h \cdot \gamma \cdot \tau_f = \frac{p_h}{m_h} \cdot \tau_f. \quad (2)$$

If one chooses the formation time to be  $\tau_f = 0.8$  fm/c, the formation length in the rest frame of the nucleus will be about 30 fm for a 5 GeV pion and about 7 fm for a 5 GeV Kaon or a 7 GeV  $\rho$  meson. These lengths have to be compared with the typical size of nuclear radii, e.g. 2.7 fm for  $^{12}\text{C}$  and 7.1 fm for  $^{208}\text{Pb}$ . The formation time has therefore a big effect on photonuclear production cross section at high energies.

To extract informations about the formation time one needs a realistic description of the final state interactions (FSI) of the reaction products. Since photon induced reactions are known to be shadowed ( $\sigma_{\gamma A} < A\sigma_{\gamma N}$ ) above  $E_\gamma \approx 1$  GeV [1, 2, 3], one also needs a way to account for this shadowing effect in photoproduction. This is straight forward within Glauber theory [4] but in simple Glauber theory the FSI are purely absorptive. A more realistic coupled channel description of the FSI is possible within a transport model. We use a semi-classical transport model based on the Boltzmann-Uehling-Uhlenbeck (BUU) equation to describe the FSI. Originally developed to describe heavy ion collisions [5] at SIS energies it has been extended in later works to investigate also inclusive particle production in heavy ion collisions up to 200 AGeV and  $\pi$  [6] and  $p$  induced as well as photon and electron induced reactions in the resonance region [7]. Inclusive photoproduction of mesons at energies between 1 and 7 GeV has been investigated in [8]. An attractive feature of this model is its capability to describe a large variety of different reaction types. However it is not clear how to account for coherence length effects such as

shadowing in a semi-classical transport model. A first attempt has been made in [8], in the next section we present a new, better way to implement shadowing in our model.

## 2 Model

Within our model we can only calculate the incoherent part of the photon nucleus cross section and we use Glauber theory to calculate coherent processes such as, e.g., coherent vector meson photoproduction. Note that the main part of the difference between the nuclear photoabsorption cross section and the incoherent photoproduction cross section at large energies stems from coherent  $\rho^0$  photoproduction. For a detailed discussion of the used transport model and the way how to implement the shadowing effect we refer to [9] and [10]. In our model the reaction of a high energy photon with a nucleus takes place in two steps. In the first step the photon reacts with one nucleon inside the nucleus (impulse approximation) and produces some final state  $X$ . In this process nuclear effects like Fermi motion, binding energies and Pauli blocking of the final state nucleons are taken into account. In the second step the final state  $X$  is propagated within the transport model. Except for the exclusive vector meson and exclusive strangeness production (see [8]) we use the Lund string model FRITIOF [11] in our model to describe high energy photoproduction on the nucleon. The particle production in FRITIOF can be decomposed into two parts. First there is a momentum transfer taking place between the two incoming hadrons leaving two excited strings with the quantum numbers of the initial hadrons. After that the two strings fragment into the observed particles. As a formation time we use 0.8 fm/c in the rest frame of each hadron; during this time the hadrons do not interact with the rest of the system. Since FRITIOF does not accept photons as incoming particles we use vector meson dominance (VMD) [12]

$$|\gamma\rangle = \left(1 - \sum_{V=\rho,\omega,\phi} \frac{e^2}{2g_V^2}\right) |\gamma_0\rangle + \sum_{V=\rho,\omega,\phi} \frac{e}{g_V} |V\rangle \quad (3)$$

and pass the photon as a massless  $\rho^0$ ,  $\omega$  or  $\phi$  with a probability corresponding to the strength of the vector meson coupling to the photon times its nucleonic cross section.

In Glauber theory shadowing of incoherent meson photoproduction arises from the interference between the two amplitudes depicted in Fig. 1. The left amplitude corresponds to the process where the photon directly produces the meson  $X$  at nucleon  $j$ . The second amplitude of order  $\alpha_{em}$  shows the process where the photon first produces a vector meson  $V$  on nucleon  $i$  without excitation of the nucleus. This vector meson then propagates at fixed impact parameter  $\vec{b}$  (eikonal approximation) to nucleon  $j$  to produce the final state meson  $X$  and leaving the nucleus in the same excited state as in the left amplitude. The FSI of the outgoing meson  $X$  are usually treated via a purely absorptive optical potential and lead to an exponential damping of the nuclear production cross section  $\sim \exp[-\sigma_X \int_{z_j}^{\infty} dz n(\vec{b}, z)]$ . If one knew the amplitudes  $T(\gamma N \rightarrow XN)$  and  $T(VN \rightarrow XN)$  one would just have to replace the purely absorptive FSI by our transport model. However, these amplitudes are in general unknown. To account for shadowing within our model we, therefore, start from (3) and use Glauber theory [4] to calculate how the single  $V$  components of the photon change due to multiple scattering on the way to nucleon  $j$  where the state  $X$

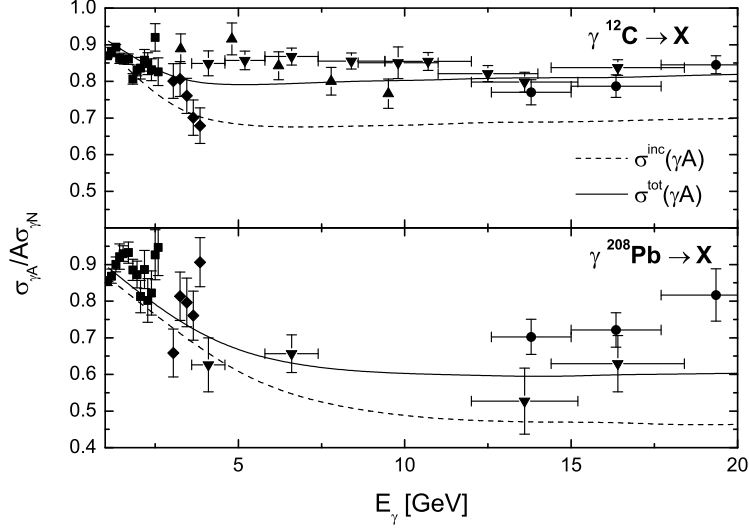


Figure 2: The nuclear photoabsorption cross section  $\sigma_{\gamma A}$  divided by  $A\sigma_{\gamma N}$  plotted versus the photon energy  $E_\gamma$ . The solid line represents the result of Reference [2] and the dashed line shows the incoherent part calculated using Eq. (6). More than 90% of the difference is due to coherent  $\rho^0$  photoproduction.

is produced:

$$|\gamma(\vec{r}_j)\rangle = \left(1 - \sum_{V=\rho,\omega,\phi} \frac{e^2}{2g_V^2}\right) |\gamma_0\rangle + \sum_{V=\rho,\omega,\phi} \frac{e}{g_V} (1 - \overline{\Gamma}_V(\vec{r}_j)) |V\rangle. \quad (4)$$

Here  $\Gamma_V(\vec{r})$  denotes the (photon energy dependent) nuclear profile function. The cross section for the photon to react with nucleon at position  $\vec{r}$  inside the nucleus can be deduced via (4) from the optical theorem

$$\sigma_{\gamma N}(\vec{r}) = \left(1 - \sum_{V=\rho,\omega,\phi} \frac{e^2}{2g_V^2}\right)^2 \sigma_{\gamma_0 N} + \sum_{V=\rho,\omega,\phi} \left(\frac{e}{g_V}\right)^2 |1 - \overline{\Gamma}_V(\vec{r})|^2 \sigma_V. \quad (5)$$

Like for the photon in vacuum each term gives the relative weight for the corresponding photon component to be passed to FRITIOF. When integrated over the whole nucleus one gets from Eq. (5) the total incoherent photonuclear cross section

$$\sigma_{\gamma A}^{\text{inc}} = \int d^3 r_j n(\vec{r}_j) \sigma_{\gamma N}(\vec{r}_j) \quad (6)$$

which is shown in Fig. 2 together with the total nuclear photoabsorption cross section as calculated in [2]. More than 90% of the difference between those two cross sections stems from coherent  $\rho^0$  photoproduction. In Fig. 3 we show how strongly the  $\rho^0$  and the  $\phi$  component of a real 20 GeV photon are shadowed in

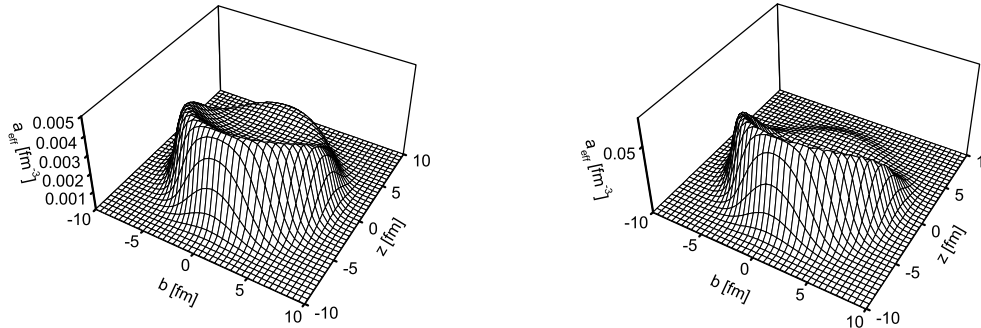


Figure 3: The number density of nucleons that react with the  $\phi$  component (*left side*) and  $\rho^0$  component (*right side*) of a 20 GeV photon for  $^{208}\text{Pb}$  calculated using Eq. (7). In both cases the nucleons on the front side of the nucleus shadow the downstream nucleons. This effect is stronger for the  $\rho^0$  component because of its larger nucleonic cross section.

Pb. We plot

$$a_{eff}^V(\vec{r}_j) = n(\vec{r}_j) \frac{1}{\sigma_{\gamma N}} \left( \frac{e}{g_V} \right)^2 |1 - \overline{\Gamma}_V(\vec{r}_j)|^2 \sigma_V \quad (7)$$

as a function of  $\vec{r}_j$ . One clearly sees that due to its smaller nucleonic cross section the  $\phi$  component is less shadowed than the  $\rho^0$  component at the backside of the nucleus. This means that strangeness production (e.g.  $K$  production), where the primary reaction is preferably triggered by the  $\phi$  component of the photon, is less shadowed than for instance inclusive  $\pi$  production. This dependence of the strength of shadowing on the reaction type is new compared to the shadowing in [8] and can also be seen directly from the second amplitude in Fig. 1 because of the occurrence of the scattering process  $VN \rightarrow XN$  at nucleon  $j$ .

As already mentioned above the purely absorptive FSI of the Glauber model are very different from the coupled channel description of a transport model. The transport model we use is based on the BUU equation that describes the time evolution of the phase space density  $f(\vec{r}, \vec{p}, t)$  of particles that can interact via binary reactions. In our case these particles are the nucleons of the target nucleus as well as the baryonic resonances and mesons ( $\pi, \eta, \rho, K, \dots$ ) that can either be produced in the primary  $\gamma N$  reaction or during the FSI. For particles of type  $i$  the BUU equation looks as follows:

$$\left( \frac{\partial}{\partial t} + \frac{\partial H}{\partial \vec{r}} \frac{\partial}{\partial \vec{r}} - \frac{\partial H}{\partial \vec{r}} \frac{\partial}{\partial \vec{p}} \right) f_i(\vec{r}, \vec{p}, t) = I_{coll}[f_1, \dots, f_i, \dots, f_M]. \quad (8)$$

In the case of baryons the Hamilton function  $H$  includes a mean field potential which in our model depends on the particle position and momentum. The collision integral on the right hand side accounts for the creation and annihilation of particles of type  $i$  in a collision as well as elastic scattering from one position in phase space into another. For fermions Pauli blocking is taken into account in  $I_{coll}$  via Pauli factors. For each particle type  $i$  such a BUU equation exists; all are coupled via the mean field and the

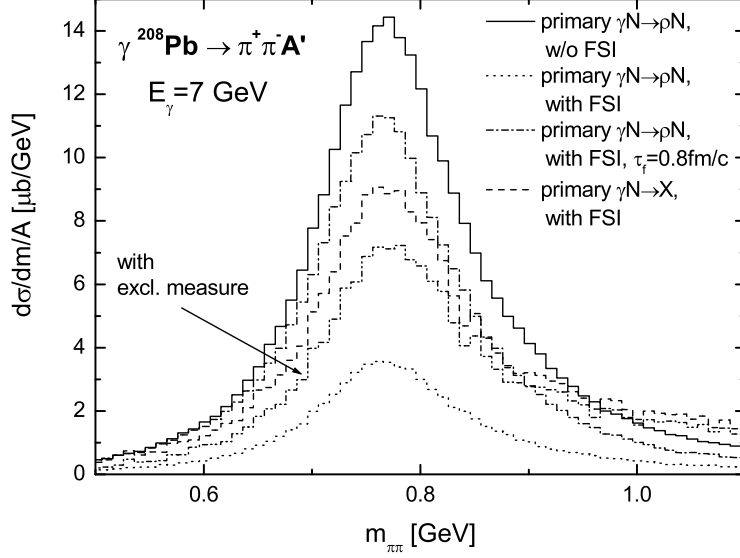


Figure 4: Mass differential cross section for exclusive  $\rho^0$  production on  $^{208}\text{Pb}$  at  $E_\gamma = 7$  GeV. The meaning of the different curves is explained in detail in the text. All the curves, except the one with the explicitly given formation time  $\tau_f = 0.8$  fm/c have been calculated with  $\tau_f = 0$ .

collision integral. This leads to a system of coupled differential-integral equations which we solve via a test particle ansatz for the phase space density

$$f_i(\vec{r}, \vec{p}, t) = \frac{1}{N} \sum_j \delta(\vec{r} - \vec{r}_j) \delta(\vec{p} - \vec{p}_j). \quad (9)$$

For a system of non interacting particles ( $I_{coll} = 0$ ) this leads directly to the classical equations of motion for the test particles:

$$\frac{d\vec{r}_j}{dt} = \frac{\partial H}{\partial \vec{p}_j} \quad \frac{d\vec{p}_j}{dt} = -\frac{\partial H}{\partial \vec{r}_j}. \quad (10)$$

Since the collision integral also accounts for particle creation in a collision the observed outgoing particle  $X$  cannot only be produced in the primary reaction but can also be created by side feeding in which a particle  $Y$  is created first which propagates and then, by FSI, produces  $X$ . In addition the state  $X$  might get absorbed on its way out of the nucleus but be fed in again in a later interaction. Both cases can a priori not be ignored but are usually neglected in Glauber models.

### 3 Results

Exclusive vector meson photo- and electroproduction on nuclei is an ideal tool to study the effects of the coherence length, formation time and color transparency. It has been investigated at HERMES [13] at photon energies between 10 GeV and 20 GeV and  $Q^2 \lesssim 5 \text{ GeV}^2$ .

The calculations for meson production on nuclei are usually done within simple Glauber theory [14]. As already mentioned above the FSI in Glauber theory are usually purely absorptive. This means that for the reaction  $\gamma A \rightarrow \rho^0 A^*$  the primary reaction has to be  $\gamma N \rightarrow \rho^0 N$ . If one treats the FSI via an absorptive optical potential one gets an exponential damping  $\sim \exp[-\sigma_{\rho N} \int_{z_j}^{\infty} dz n(\vec{b}, z)]$  of the nuclear production cross section. Up to now we can, for technical reasons, perform calculations only for real photons up to an energy of about 7 GeV. In Fig. 4 we show the results for the mass differential cross section of incoherent  $\rho^0$  photoproduction on  $^{208}\text{Pb}$  for  $E_\gamma = 7 \text{ GeV}$ . The solid line represents a calculation where the primary reaction is  $\gamma N \rightarrow \rho^0 N$ . It already includes the effects of shadowing, Fermi motion, Pauli blocking and the nucleon potential, but no FSI. The dotted line shows the effect of the FSI without a formation time of the  $\rho^0$  in  $\gamma N \rightarrow \rho^0 N$ . The simple Glauber model yields exactly the same result, which means that FSI processes like ( $\rho^0 N \rightarrow \pi N$ ,  $\pi N \rightarrow \rho^0 N$ ) where the primary  $\rho^0$  gets absorbed first and is fed into the outgoing channel by a later FSI are negligible. If one assumes a formation time of  $\tau_f = 0.8 \text{ fm}/c$  for the  $\rho^0$  one gets the result indicated by the dash-dotted line. Due to the finite formation time there is less absorption and the nuclear production cross section increases. If the spectrum looked like this one would in Glauber theory be lead to the conclusion of a finite  $\rho^0$  formation time.

However, one will get a similar result with  $\tau_f = 0$  if one allows for other primary reaction besides  $\gamma N \rightarrow \rho^0 N$  and uses a coupled channel model. This can be seen by looking at the dashed line in Fig. 4. In this case one finds that the main part of the additional  $\rho^0$  stem from inclusive  $\rho^0$  production in the primary event, e.g.  $\gamma N \rightarrow \rho^0 \pi N$  where the  $\pi$  gets absorbed during the FSI. One could now apply an exclusivity measure like in the HERMES experiment

$$\Delta E = \frac{P_Y^2 - M_N^2}{2M_N}, \quad (11)$$

where  $P_Y$  denotes the 4-momentum of the undetected final state and  $M_N$  is the nucleon mass, with  $-2 \text{ GeV} < \Delta E < 0.6 \text{ GeV}$ . This leads to a decrease of the cross section (dash-dot-dotted line) because some of the inclusive primary events are excluded. If the exclusivity measure was good enough to single out only the exclusive primary events, the curve would coincide with the dotted line and Glauber theory would be applicable. Since this is not the case, one still extracts an incorrect formation time when using simple Glauber theory. One therefore needs an additional constraint to make Glauber theory applicable. This becomes clear by examining the differential cross section  $\frac{d\sigma}{dt}$  in Fig. 5. The meaning of the lines are as before. One can see that for  $|t| > 0.1 \text{ GeV}^2$  the full calculation with exclusivity measure (dash-dot-dotted line) gives the same result as the one with the primary reaction  $\gamma N \rightarrow \rho^0 N$  and FSI (dotted line). This means that only in this kinematic region Glauber theory can be used. In the HERMES experiment one makes a lower  $|t|$  cut to get rid of the  $\rho^0$  stemming from coherent  $\rho^0$  photoproduction. In the case of lead and  $E_\gamma = 7 \text{ GeV}$  the coherent part can be neglected above  $|t| = 0.05 \text{ GeV}^2$ . If one wants to apply Glauber theory one will need to increase this threshold to approximately  $|t| = 0.1 \text{ GeV}^2$  to suppress

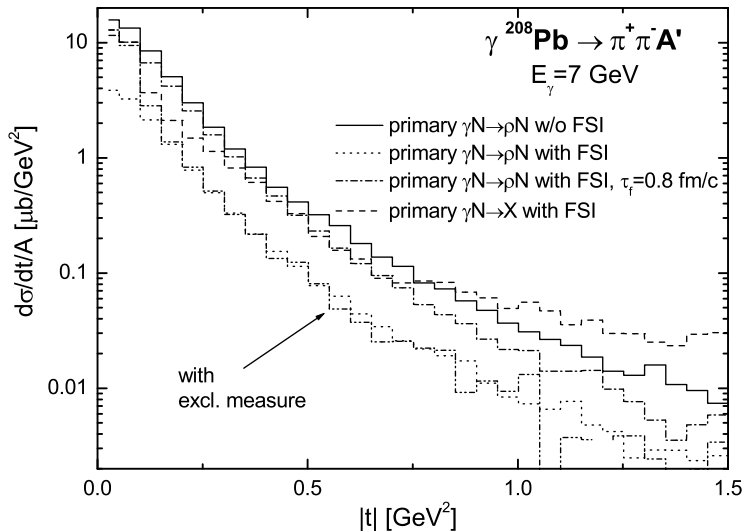


Figure 5: Calculated  $\frac{d\sigma}{dt}$  for exclusive  $\rho^0$  production on  $^{208}\text{Pb}$  at  $E_\gamma = 7$  GeV. The meaning of the different curves is the same as in Fig. 4.

contributions from inclusive  $\rho^0$ .

One sees that Glauber theory can be trusted only under certain kinematic constraints. To describe less exclusive reactions one needs a more realistic description of the FSI. In Fig. 6 we show the cross section for the reactions  $\gamma A \rightarrow K^+ X$  and  $\gamma A \rightarrow K^- X$  in the photon energy range 1-7 GeV for  $^{12}\text{C}$  and  $^{208}\text{Pb}$  which has already been investigated in [8]. The solid curve in Fig. 6 represents the results of the full calculation (including shadowing, FSI,  $\tau_f = 0.8$  fm/c, etc.). By comparison with the calculation without shadowing (dash-dotted line) one sees how important shadowing becomes at high energies. At 7 GeV it reduces the nuclear production cross section to about 75% for Carbon and 65% for Lead. The importance of a full coupled channel treatment of the FSI becomes clear when looking at inclusive  $K^+$  production. Since the  $\bar{s}$  quark cannot be absorbed in medium the FSI can just increase the  $K^+$  production via processes like  $\pi N \rightarrow K^+ Y$  ( $Y = \Sigma, \Lambda$ ) for example. This one finds by comparison with the calculation without FSI (dashed line). As a consequence of this, a shorter formation time will lead to an increase of the  $K^+$  production cross section as can be seen from the dotted line. The reason is that with decreasing formation time the primarily produced pions have a greater chance to produce  $K^+$  in the FSI. As already mentioned in the introduction for  $\tau_f = 0.8$  fm/c the formation length of fast pions is larger than the nuclear dimension, so that they will leave the nucleus without further scattering. An enhancement of the  $K^+$  production cross section due to FSI can of course not be explained by purely absorptive FSI as in simple Glauber theory. The  $K^-$  can also be absorbed via processes like  $K^- N \rightarrow \pi Y$ . This effect compensates the production due to FSI in  $^{12}\text{C}$  and dominates in  $^{208}\text{Pb}$  as can be seen in Fig. 6.



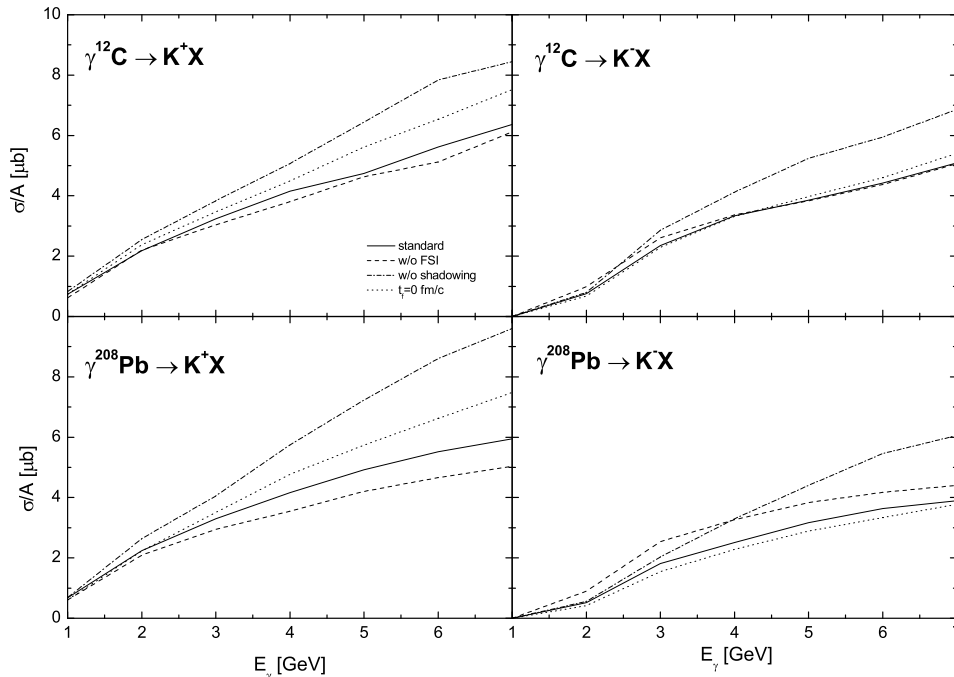


Figure 6: Photoproduction cross section for  $K^+$  (left) and  $K^-$  (left) for  $^{12}\text{C}$  and  $^{208}\text{Pb}$  plotted as a function of the photon energy. The solid line represents the full calculation. The dash-dotted line shows the result without shadowing of the incoming photon, the dashed line the result without FSI and the dotted line the calculation without formation time.

## 4 Summary & Outlook

We have shown that high energy photoproduction off nuclei offers a great possibility to study the physics of hadron formation. However, one needs a reliable model of the FSI to extract the formation time from the production cross sections. Whereas Glauber models allow for a straight forward implementation of the nuclear shadowing effect they usually have the disadvantage of a purely absorptive treatment of the FSI. As we have shown the latter might lead to a wrong estimate of the formation time if the kinematic cuts are not chosen properly. A more realistic treatment of the FSI is possible within a coupled channel transport model. However in such a model it is not totally clear how to account for the shadowing effect. We have presented a method to account for these coherence length effects which can easily be extended to higher energies and virtual photons. This will be done in future work so that we can study the effects of formation time and color transparency in particle production in the HERMES regime [13, 15]. We will also investigate charm production since we expect the same FSI effect as observed for the  $K^+$  also for the  $\bar{D}$ . In addition, we plan to implement a more realistic time dependence of the cross section for the produced particles during their evolution which might again modify the extracted formation time.

## 5 Acknowledgments

This work was supported by DFG.

## References

- [1] N. Bianchi *et al.*, Phys. Rev. C **54**, 1688 (1996); V. Muccifora *et al.*, Phys. Rev. C **60**, 064616 (1999).
- [2] T. Falter, S. Leupold and U. Mosel, Phys. Rev. C **62**, 031602 (2000).
- [3] T. Falter, S. Leupold and U. Mosel, Phys. Rev. C **64**, 024608 (2001).
- [4] R. J. Glauber, in *Lectures in Theoretical Physics*, edited by W.E. Brittin and L.G. Dunham (Wiley Interscience, New York, 1959), Vol. I, p. 315; D. R. Yennie, in *Hadronic Interactions of Electrons and Photons*, edited by J. Cummings and H. Osborn (Academic, New York/London, 1971), p. 321.
- [5] B. Blättel, V. Koch and U. Mosel, Rept. Prog. Phys. **56**, 1 (1993); G. Wolf, W. Cassing and U. Mosel, Nucl. Phys. A **552**, 549 (1993); S. Teis, W. Cassing, M. Effenberger, A. Hombach, U. Mosel and G. Wolf, Z. Phys A **356**, 421 (1997); A. Hombach, W. Cassing, S. Teis and U. Mosel, Eur. Phys. J. A **5**, 157 (1999).
- [6] M. Effenberger, E. L. Bratkovskaya, W. Cassing and U. Mosel, Phys. Rev. C **60**, 027601 (1999).
- [7] M. Effenberger, A. Hombach, S. Teis and U. Mosel, Nucl. Phys. A **614**, 501 (1997); J. Lehr, M. Effenberger and U. Mosel, Nucl. Phys. A **671**, 503 (2000).
- [8] M. Effenberger and U. Mosel, Phys. Rev. C, **62**, 014605 (2000).
- [9] M. Effenberger, E. L. Bratkovskaya and U. Mosel, Phys. Rev. C **60**, 044614 (1999).
- [10] T. Falter and U. Mosel, in preparation.
- [11] B. Anderson, G. Gustafson and Hong Pi, Z. Phys. C **57**, 485 (1993).
- [12] T. H. Bauer, F. Pipkin, R. Spital and D. R. Yennie, Rev. Mod. Phys. **50**, 261 (1978).
- [13] K. Ackerstaff *et al.*, Phys. Rev. Lett. **82**, 3025 (1999).
- [14] J. Hüfner, B. Kopeliovich and J. Nemchik, Phys. Lett. B **383**, 362 (1996); J. Hüfner and B. Kopeliovich, Phys. Lett. B **403**, 128 (1997); R. Engel, J. Ranft and S. Roesler, Phys. Rev. D **55**, 6957 (1997); G. Kerley and G. Shaw, Phys. Rev. D **56**, 7291 (1997); A. Pautz and G. Shaw, Phys. C **57** 2648 (1998); T. Renk, G. Piller and W. Weise, Nucl. Phys. A **689**, 869 (2001).
- [15] A. Airapetian *et al.*, Eur. Phys. J. C **20**, 479 (2001).